

Molecular dynamics of the α -relaxation during crystallization of a low-molecular-weight compound: A real-time dielectric spectroscopy study

J. Dobbertin,^{a)} J. Hannemann, and C. Schick

University of Rostock, Department of Physics, Universitätsplatz 3, 18051 Rostock, Germany

M. Pötter and H. Dehne

University of Rostock, Department of Chemistry, Buchbinderstr. 9, 18051 Rostock, Germany

(Received 9 October 1997; accepted 23 February 1998)

Low-molecular-weight compounds often crystallize to systems with 100% crystallinity. There are only a few examples where a small amorphous fraction, characterized by a glass transition, remains after long time crystallization from the melt. The crystallization of such a glass-forming low-molecular-weight compound was investigated in order to monitor the change of the molecular dynamics with increasing crystallinity by dielectric spectroscopy and differential scanning calorimetry (DSC). The measurement of the dielectric α -relaxation was performed in real time during isothermal crystallization above the glass transition. At high crystallinities (above 90%) a shift of the peak position and a broadening of the dielectric spectrum was observed. The calorimetric glass transition temperature shifts in the same region for about 15 K to higher temperatures. No direct information about the morphology of the samples is available at the moment but indirect measurements indicate a layerlike crystalline structure. Then the remaining amorphous fraction can be considered between the crystal layers and the observed changes in the relaxation behavior may be caused by spatial confinement in the order of nanometer. © 1998 American Institute of Physics. [S0021-9606(98)50321-2]

I. INTRODUCTION

The glass transition as an universal phenomenon can be observed not only in amorphous but also in semicrystalline systems. The molecular dynamics in semicrystalline polymers are described in several publications.^{1,2} Only few papers³ exist dealing with the relaxation behavior in semicrystalline low-molecular-weight compounds. In contrast to polymers, it is difficult to fix a semicrystalline structure and to measure the dynamics in the remaining noncrystalline part above their calorimetric glass transition temperature, T_g . In most cases such sterically simple structures result in a full crystallization of the sample. Therefore only few details are known about the influence of the crystalline structure and of possible spatial confinement on the relaxation behavior in low-molecular-weight compounds.

The investigation of the dynamic glass transition (α -relaxation) during the crystallization should help to enlighten the influence of crystallinity on the relaxation process. In literature some real time crystallization studies of polymers are described.^{4,5} Inspired by these experiments, we made the similar investigations at a low-molecular-weight compound. The reason for our investigations is to answer the question whether the crystalline morphology influences the α -relaxation in polymers and in nonpolymeric compounds differently.

The morphology of polymers is mainly determined by the chain structure of the molecules. Crystallization in polymers often stops at crystallinities of about 40% because of

entanglements and other noncrystallizable parts of the chain near the growing crystal. In contrast to low-molecular-weight compounds, polymers do not crystallize to a simple two-phase system. In addition to the crystalline and the melt like amorphous part a rigid amorphous fraction must be introduced.⁶ On this way the observation that there is not always a one-to-one relationship between crystallinity and the step in heat capacity in the glass transition region can be understood. The observed deviations are thought to be caused by molecules whose mobility is somehow hindered (rigid amorphous), even though they are entirely or partially located within the amorphous phase.⁷

To distinguish between the influence of the rigid amorphous fraction (chain structure) with restricted molecular mobility and spatial confinement effects on the relaxation behavior in semicrystalline polymers is very difficult. It seems easier to study semicrystalline samples showing a simple two phase behavior. In order to do this, we investigate the α -relaxation during crystallization of a low-molecular-weight compound. In such glass-forming systems a rigid amorphous fraction, typical for long chain molecules, does not exist. Low-molecular-weight compounds often crystallize to a sample with 100% crystallinity. With increasing crystallinity the dimension of the remaining amorphous matrix decreases. Because spatial confinement effects for the α -relaxation are expected at dimensions below 10 nm (Refs. 8, 9) the final states of crystallization just before contact between growing crystals is of special interest. In the case of a sample with possible 100% crystallinity this state exists only for a short time and there are other amorphous regions with much bigger dimensions at the same time. The latter

^{a)}Electronic mail: joergen.dobbertin@physik.uni-rostock.de

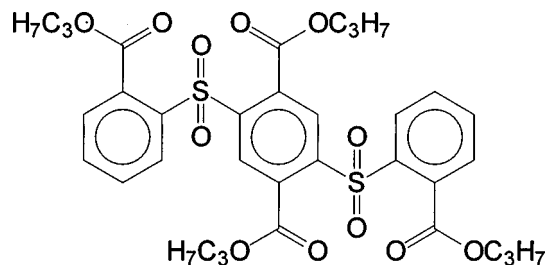


FIG. 1. 2,5-Bis-(2-propyloxycarbonyl-phenylsulfonyl) terephthalic acid dipropyl ester.

will determine the observed relaxation behavior. To study spatial confinement in low-molecular-weight compounds therefore needs samples with remaining amorphous regions between the crystals. There are only few examples where such amorphous fraction, characterized by a glass transition, remains after long time crystallization from the melt.³ The crystallization of such a glass-forming low-molecular-weight compound was investigated in order to monitor the change of the molecular dynamics with increasing crystallinity by dielectric spectroscopy and differential scanning calorimetry (DSC). Finally, the observations give some hints which effects are due to spatial confinement in a semicrystalline sample and which are caused by the chain structure of polymers.

II. EXPERIMENT

A. Sample

A glass-forming low-molecular-weight compound of the novel sulfur ligated trilling type (Fig. 1) was investigated. The synthesis of compounds with structure analogs are described in Ref. 10. This compound was chosen because a small amount of noncrystalline material remains after isothermal crystallization. This seems to be due to the crystallization in a layer structure, as detailed below.

An other reason for choosing this sample is due to its high dielectric relaxation intensity for the α -relaxation. So it is possible to investigate the relaxation process up to high crystallinity where the relaxation intensity decreases nearly two orders of magnitude.

The parameters at the melting point were taken from the first DSC scan for the crystals from the synthesis and the glass transition parameters were determined at the second heating run after cooling with 10 K/min, see below (Table I).

B. Dielectric measurements

The dielectric relaxation measurements were performed with a BDS 4000 system from Novocontrol GmbH. This experimental setup uses a frequency response analyzer SI

1260 (Solatron-Schlumberger), which is supplemented by a high-impedance preamplifier of variable gain.¹¹ The sample was prepared by melting the substance between two condenser plates (16 mm in diameter) and quenching below glass temperature. The sample with a thickness of 50 μm (fixed by Kapton spacers) was kept in a cryostat where the sample temperature was controlled by using a nitrogen gas stream of controlled temperature. Frequency scans were performed at constant temperature, with a temperature stability better than 0.1 K.

The measured frequency sweeps can be described quantitatively by generalized relaxation functions. The most general one is the Havriliak–Negami (HN) equation¹²

$$\epsilon^*(f) = \epsilon_\infty + \frac{\epsilon_{st} - \epsilon_\infty}{(1 + (if/f_{HN})^\beta)^\gamma} \quad (0 < \beta, \beta\gamma \leq 1). \quad (1)$$

β and γ are shape parameters; f is the frequency of the applied field; f_{HN} the characteristic frequency; and, $\Delta\epsilon = \epsilon_{st} - \epsilon_\infty$ the relaxation strength or intensity [$\epsilon_{st} = \epsilon'(f)$ for $f \ll f_{HN}$; $\epsilon_\infty = \epsilon'(f)$ for $f \gg f_{HN}$]. The characteristic frequency f_{HN} resulting from the fitting procedure depends on some extent on the chosen shape parameters β and γ . The frequency of the maximum dielectric loss f_{max} is not influenced by the shape parameters and has been used in the following as the relaxation frequency. At the low frequency tail the conductivity must be included in the fitting procedure.¹³

C. Calorimetric measurements

For the calorimetric measurements a Perkin–Elmer DSC-2 differential scanning calorimeter was used. The temperature scale of the calorimeter was calibrated with indium and lead for the scanning rate used and for the heat flow by sapphire. The purge gas was nitrogen. The temperature of the calorimeter block were kept well stabilized at temperatures of (200 ± 0.1) K in order to reach reproducible scans. Sample mass was about 15 mg and the scanning rate was 10 K/min for all heating and cooling cycles. The calorimetric glass transition temperature was determined in the heating cycle as the temperature at the half step in c_p .

III. RESULTS

A. Dielectric relaxation of the amorphous low-molecular-weight-compound

A temperature sweep at constant frequency shows two dielectric relaxation phenomena (Fig. 2). At high temperatures a strong relaxation exists which is related to the thermal vitrification process and called α -relaxation. Below the thermal glass transition temperature a weak low temperature relaxation occurs, called β -relaxation (secondary or Johari–Goldstein¹⁴ process).

To determine the temperature–time (frequency) dependence of the relaxation processes, frequency sweeps at isothermal conditions were performed. The peak position of the α -relaxation follows a Vogel–Fulcher–Tammann (VFT) equation

$$\lg f_{max} = A - \frac{B}{T - T_0}. \quad (2)$$

TABLE I. Results from thermal and structural analysis.

T_m (K)	ΔH_m (kJ/mol)	T_g (K)	Δc_p (J/mol K)	Molecular mass (calculated/measured)
410	58.3	278.9	267	$C_{34}H_{38}O_{12}S_2$ 702.79/703

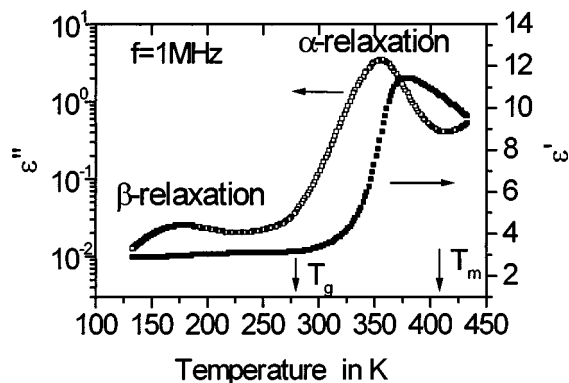


FIG. 2. Temperature sweep while cooling from the melt with 10 K/min at a constant frequency of $f = 1$ MHz.

$A = \lg f_{\infty}$ and B are constants, T_0 is the so called ideal glass transition or Vogel temperature. From the slope of the α -relaxation a fragility parameter (in the sense of Angell^{15,16}) of $m = 77$ was determined, indicating a medium fragility.

The β -relaxation follows an Arrhenius (ARR) law (VFT equation with $T_0 = 0$) which is characteristic for thermal activated processes

$$\lg f_{\max} = A - \frac{B}{T}. \quad (3)$$

The parameters of both relaxation processes are listed in Fig. 3.

B. Real time dielectric measurements during crystallization

Frequency sweeps from 3 MHz to 100 Hz were performed during the isothermal crystallization process at different times. For the melt-crystallization (mc), shown in Fig. 4, the sample was heated above the melting temperature and then cooled down to the crystallization temperature of 343 K

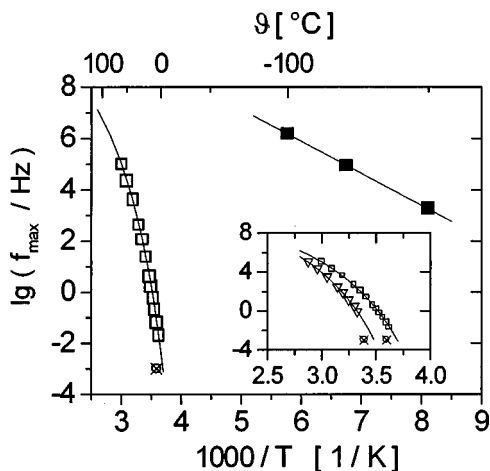


FIG. 3. Temperature dependence of the frequency position of α - (\square) and β - (\blacksquare) relaxation. Solid lines are fits with the VFT ($A = 11.91$, $B = 803.9$ K, $T_0 = 216.8$ K) and ARR [$A = 13.37$, $B = 1247$ K ($E_a = 23.9$ kJ/mol)] equation. \otimes is the calorimetric glass temperature at a heating rate of 10 K/min which corresponds to a frequency of about 10^{-3} Hz. The inset shows the α -relaxation for the amorphous (\square) and the semicrystalline sample (∇), crystallized for 15 h at 343 K, $\chi_c = 98\%$.

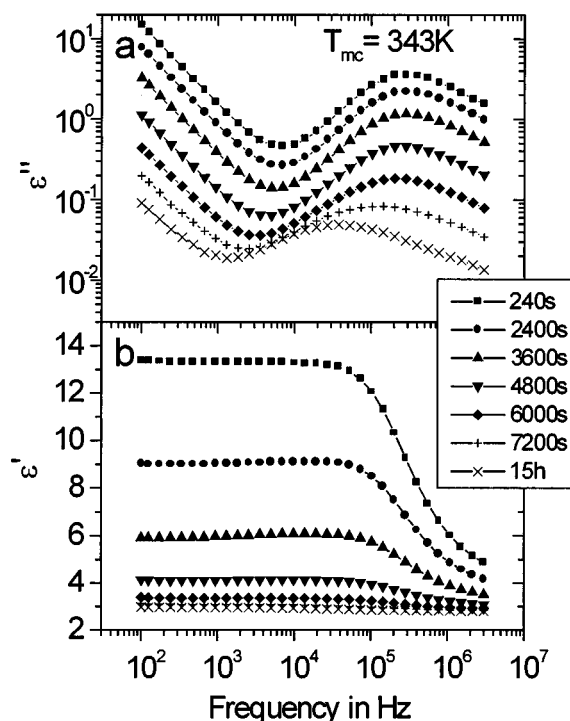


FIG. 4. Real (b) and imaginary part (a) of the complex dielectric function for the α -relaxation during isothermal crystallization at selected crystallization times.

with a cooling rate of about 5 K/min. To get isothermal conditions a temperature setting time of about 5 min was necessary. After this time the first sweep was started. Each measurement requires about 240 s. Although this was a long time for such experiments no crystallization during one measurement sweep can be observed [there is no decrease of ϵ' to lower frequencies for the frequency sweep started at 3 MHz, see Fig. 4(b)].

For comparison, a cold-crystallization (cc) at 333 K was also performed under the same measuring conditions. The sample was cooled down from the melt below the calorimetric glass transition temperature, T_g , and then heated up to the cold-crystallization temperature T_{cc} of 333 K. The heating and cooling rate was about 5 K/min. There are no qualitative differences in the results from the melt-crystallization and the cold-crystallization so that we use, in the following, only the results from the melt-crystallization.

Figure 4 shows the real time evolution of the α -relaxation during the isothermal crystallization process at $T_{mc} = 343$ K. The crystallization time is marked on the right-hand side of the figure. During crystallization proceeds three features are observed:

- Reduction of the intensity of the α -process with increasing crystallization time but with nonzero intensity after a 15 h crystallization;
- shift of the α -loss peak to lower frequencies;
- change of the shape of the dielectric spectrum.

After a 15 h crystallization at 343 K a relaxation peak, with a relaxation strength of about 2% of that of the amorphous sample, can still be observed. This indicates that the sample

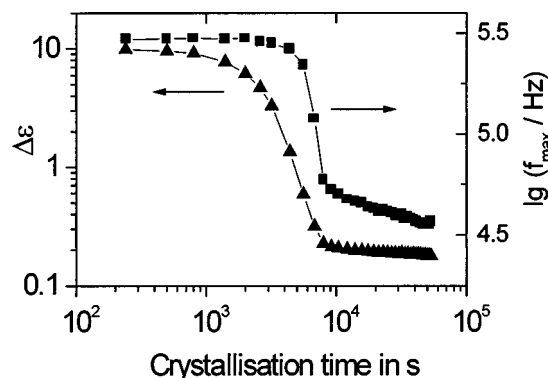


FIG. 5. Relaxation intensity (▲) and peak position (■) as a function of crystallization time during isothermal crystallization at 343 K.

does not crystallize to 100%. The remaining relaxation process shows a VFT behavior, typical for an α -relaxation. In comparison to the fully amorphous sample, the α -relaxation is shifted for about 15 K to higher temperatures (see inset in Fig. 3).

Relaxation intensity, $\Delta\epsilon$, and peak position, f_{\max} , as a function of crystallization time are shown in Fig. 5. For $\Delta\epsilon$ a logarithmic scale was used, to show the reduction of nearly two orders of magnitude and the small changes at the very end of crystallization.

C. Determination of crystallinity

It is known that low-molecular-weight compounds crystallize normally to a two phase system. That means only amorphous and crystalline parts have to be taken into account. This is somewhat different from polymers, where an additional noncrystalline part exists, the so-called rigid amorphous fraction, which does not participate to the glass transition.^{5,6,17,18} This seems to be important for possible differences between the dynamic glass transition of semicrystalline polymers and low-molecular-weight compounds. That is why we have to check the two-phase behavior for the compound under investigation. One way is to determine the relationship between the step height in the heat capacity at the glass transition, Δc_p and the heat of fusion, ΔH_m , from a DSC-scan. For a two phase system Δc_p should be proportional to $1 - \chi_c$. Besides χ_c can be determined from ΔH_m .

First the crystals from chemical synthesis (as received from recrystallization with ethanol, yielding small single crystals) were measured from 240 K to 425 K (see Fig. 6) to get the parameters for the 100% crystalline sample. Then the sample was cooled down to 343 K and annealed for a crystallization time $t_{mc} = 1$ min. After that the sample was cooled down to 240 K and the next DSC-scan to 425 K was started. Then the procedure was repeated with a longer crystallization time. From all scans the step height of heat capacity at the glass transition, Δc_p , the calorimetric glass temperature, T_g , the heat of fusion, ΔH_m , and the melting peak temperature, T_m , were determined.

Unfortunately there is a problem in the analysis of this measurement. For the crystals obtained from the recrystallization with ethanol we get a melting point of 410 K. The samples crystallized from the melt at 343 K have a melting

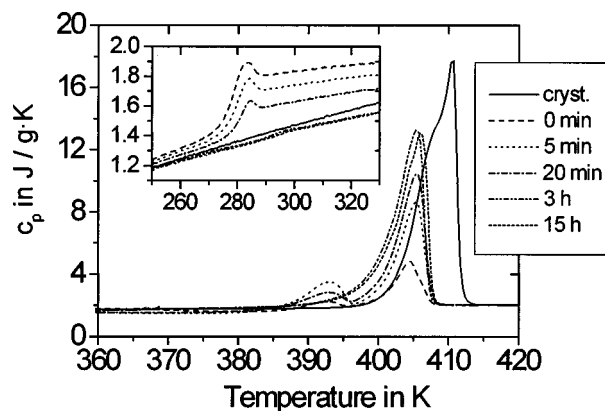


FIG. 6. DSC scans in the melting region and the glass transition region (inset) at selected crystallization times at $T_{mc} = 343$ K. The solid line indicates the first heating scan for the crystals from ethanol; the broken lines indicate the heating scans after the isothermal crystallization for different times at 343 K.

point of 405 K, indicating different crystal modification. Therefore we cannot use the heat of fusion determined for the crystals from ethanol as the value of the 100% crystalline sample for the series crystallized at 343 K from the melt.

That is why we have performed x-ray measurements (WAXS and SAXS). Compared to the crystals from ethanol the samples isothermal crystallized for 15 h at 343 K show a slightly lower (1% or 2%) crystallinity. Different crystal modifications are confirmed, too.

This result allows us to assign the heat of fusion of the sample crystallized for 15 h at 343 K ($\Delta H_m = 58$ J/g) to a crystallinity of 98% and to determine the mass crystallinity, χ_c , by $\chi_c = \Delta H_m / (58 \text{ J/g} \cdot 0.98)$ (Fig. 7).

The straight line in Fig. 7 represents the two-phase model. If there is no rigid amorphous fraction (two phase system) the whole noncrystalline part ($1 - \chi_c$) should participate in the glass transition ($\Delta c_p / \Delta c_{pa} = 1 - \chi_c$). Δc_{pa} is the step in the specific heat capacity for the amorphous sample. As shown in Fig. 7 for the compound under investigation the normalized relaxation intensity $\Delta c_p / \Delta c_{pa}$ is in good agreement with the two-phase model. That confirms the

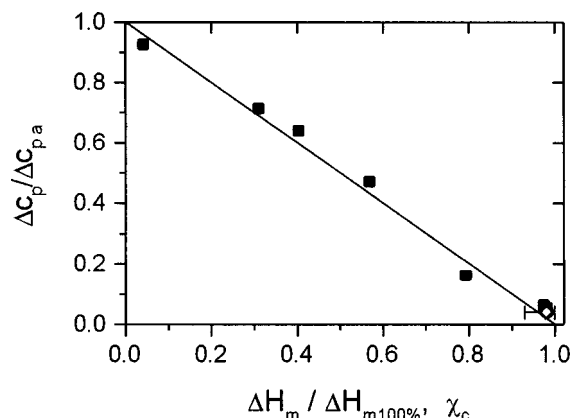


FIG. 7. Normalized step height of heat capacity at the glass transition, $\Delta c_p / \Delta c_{pa}$ vs normalized heat of fusion, $\Delta H_m / \Delta H_{m100\%}$. The open diamond \diamond represents the crystallinity determined by x-ray for the sample isothermal crystallized for 15 h.

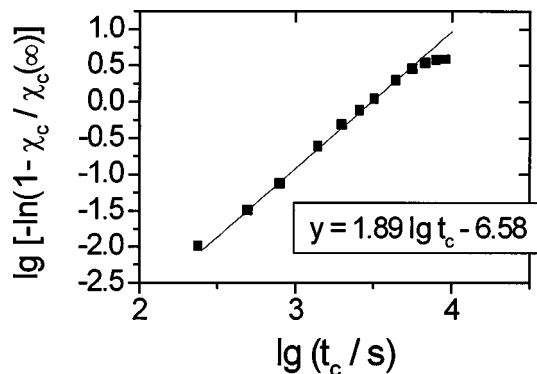


FIG. 8. Avrami plot with regression line and parameters.

assumption that for the investigated low-molecular-weight compound the whole noncrystalline part participates in the relaxation process.

The x-ray diffraction patterns are very complex and at the moment we are not able to extract some information about the arrangement of the crystalline and the amorphous regions. To obtain at least some qualitative information about the crystallization process and the possible morphology we performed an Avrami analysis¹⁹ (Fig. 8),

$$\chi_c(t)/\chi_c(\infty) = 1 - \exp(-kt^n), \quad (4)$$

or

$$\lg[-\ln(1 - \chi_c(t)/\chi_c(\infty))] = n \lg t + \lg k, \quad (5)$$

where n is a constant whose value depends on the mechanism of nucleation and form of crystal growth, and k is a constant containing the nucleation and growth parameters. $\chi_c(\infty)$ is the ultimate crystallinity at very long time (for our sample 98%).

The value of the Avrami exponent $n=1.89$ is fairly closed to the theoretical value of 2 which would indicate a two-dimensional crystal growth (under assumption of athermal nucleation).²⁰ That means we have a lamellalike structure. This is in agreement with electron micrographs obtained from structure analogues twin molecules.²¹ The remaining interface between neighboring crystals seems to be the reason for the noncrystalline part at the end of crystallization and allows an estimation of the thickness of the amorphous regions, see below.

The same analysis with a dielectric standard substance Salol yields an Avrami exponent of $n \approx 3$ which would indicate a three-dimensional crystal growth. This compound crystallize to a 100% crystalline sample.

IV. DISCUSSION

A. Variation of maximum frequency and glass temperature with crystallinity

In Fig. 5 we have shown the shift of the maximum position of the dielectric loss curve with increasing crystallization time. More instructive is the maximum frequency as a function of the degree of crystallinity as presented in Fig. 9. The degree of crystallinity can be estimated from the normal-

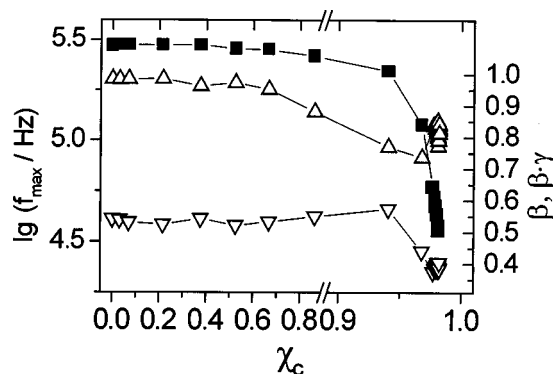


FIG. 9. Dielectric loss peak position (■), HN-shape parameters β (▲) and $\beta \cdot \gamma$ (▽) in dependence of crystallinity ($\chi_c = 1 - \Delta\epsilon/\Delta\epsilon_a$). The region from 0.9 to 1 is represented in a zoomed scale.

ized dielectric intensity [$\chi_c \approx 1 - (\Delta\epsilon/\Delta\epsilon_a)$], because the relaxation intensity is proportional to the noncrystalline part as shown above.

It is clearly visible that the shift of the α -peak position starts at a degree of crystallinity above 90%. In addition to the shift of the peak position, a decreasing of the HN shape parameters β and $\beta \cdot \gamma$ can also be observed.

It remains the question whether this is due to a shift and broadening of one peak or it is due to the result of the superposition of two processes representing parts with different molecular mobility. Consider a semicrystalline morphology build up by layerlike crystals separated by small amorphous interfaces. The reason for such an interface may be that there are molecules which cannot be incorporated into one of the neighboring crystals. Because the molecules have no chain structure, supporting the development of thicker noncrystalline layers as observed in polymers, the amorphous layer thickness is restricted to the dimension of a single molecule. In our case the longest molecule axis in the crystalline state is in the order of 1.5 nm, as determined by x-ray diffraction. Then, because of the expected very thin amorphous layers between the crystals, the volume fraction of this material is negligible as long as an amorphous matrix between the growing crystals exists. The latter also determines the relaxation behavior until the amorphous matrix disappears. In the Avrami-plot this is indicated by the deviation from the straight line for crystallization times greater than 2 h. After this time only the relaxation process in the thin amorphous layers between the crystals can be seen. This process may be influenced by the spatial confinement due to the layer thickness of less than 2 nm. The deviation from the Avrami model corresponds very well with the changes in the relaxation behavior as shown in Fig. 9 and 11, supporting this simple picture. If there are two different amorphous regions inside the semicrystalline sample during the crystallization process it should be possible to separate both at the very end of crystal growth, e.g., after 2 h crystallization (see Fig. 4).

In Fig. 10 the result of such a separation into two processes is shown. One peak has the same maximum position and curve shape as the fully amorphous sample and the other that of the sample with the highest crystallinity (Fig. 10). This indicates that during crystallization the amorphous ma-

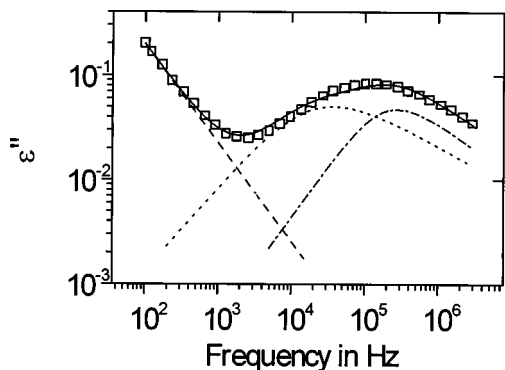


FIG. 10. Separation of the measured dielectric loss curve at a crystallization time of 2 h (\square) into two parts. Dotted line, HN-fit to the α -relaxation process in the thin amorphous layers (15 h crystallization time). Dashed dotted line, proportional to the HN-fit of the α -relaxation process in the amorphous (1.3% relaxation strength of the full amorphous sample). The solid line is the superposition of these two processes together with a conductivity term (dashed line).

trix disappears and a low frequency relaxation process can be detected. This relaxation process should be related to the interface between the lamellalike crystals and the observed relaxation behavior may be the result of a spatial confinement, as discussed below.

This result is supported by the calorimetric investigations, too. For the thermal glass transition we found the same behavior like the frequency position of the dielectric loss peak. At a crystallinity above 90% there is a step of 15 K in the calorimetric glass transition temperature without drastically changes in the curve shape (see Fig. 11). This matches well with the dielectric α -relaxation, where the isochronal loss peak for the semicrystalline sample is also shifted to a 15 K higher temperature than that of the amorphous sample, see inset in Fig. 3.

B. Comparison with the results from polymers

At first glance there are no differences between our results for a low-molecular-weight compound and the results from Ezquerro *et al.*^{4,5} for polymers. As in polymers, we found a slowing down of the α -relaxation and a broadening of the loss peak. But a quantitative analysis shows that both findings start at much higher crystallinities for the low-

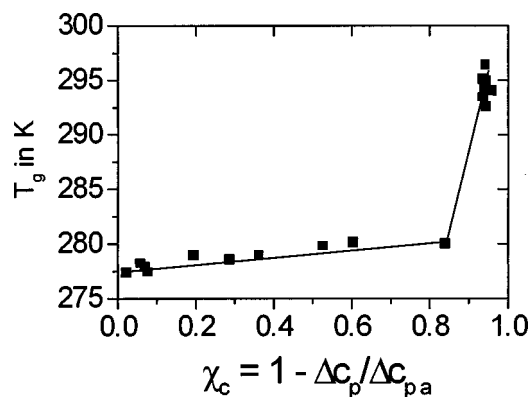


FIG. 11. Calorimetric glass transition temperature vs crystallinity.

molecular-weight compound. Also the broadening of the low frequency tail is weak compared to the effect for polymers.

Consider a layerlike crystalline structure with amorphous interfaces as well for the low-molecular-weight compound as for semicrystalline polymers. Then for both materials qualitatively the same behavior is expected. The only difference is the amount of amorphous material between the crystals. For polymers, totally filled with layer stack structures, often more than 50% amorphous material remains. For the low-molecular-weight compound we detect only about 2% amorphous material between the crystals. The observed relaxation behavior will be influenced by this interfacial material only if its fraction is comparable or smaller than the fraction of the amorphous matrix. Therefore the relaxation process in polymers is influenced at lower crystallinities compared to the situation in the low-molecular-weight compound. For the low-molecular-weight compound the small amount of interfacial material yields an influence on the relaxation behavior only at the very end of crystallization when the amount of remaining meltlike amorphous material is comparable to that of the interfacial fraction.

C. Spatial confinement

In both cases we can discuss the observed effects, slowing down and broadening of the α -relaxation, as a consequence of spatial confining. One of the open questions still behind glass transition is that of the characteristic length of the corresponding molecular motions. One way to get information about this length scale is to investigate the α -relaxation in geometries comparable with the expected length scale. The results from a large number of studies are published.²²⁻²⁷ Mainly controlled porous glasses were used to investigate the influence of size effects on relaxational dynamics. The results are conflicting. Both, a decrease^{22,23} and a small increase²⁴ in the dynamic glass transition temperature was found. Arndt *et al.*²⁵ found a strong dependence of these effects from the interaction between the glass forming compound and the confining material.

In semicrystalline materials, as discussed here, only small effects related to surface interactions should appear, because the restriction of the glass-forming regions is due to the same substance. For semicrystalline poly(ethylene terephthalate) (PET) we found a slowing down of the α -relaxation with increasing geometrical restrictions.^{28,18} Unfortunately for polymers the situation is complicated because of the chain structure and the formation of a rigid amorphous fraction. Therefore some of the observed effects may be caused by the very special morphology of semicrystalline polymers. The comparison of the results from semicrystalline low-molecular-weight compounds with that of polymers allows us to distinguish between effects caused by the chain structure and that due to spatial confinement. Unfortunately at the moment we are not able to determine the length scale of the confining geometry in the low-molecular-weight compound. From the Avrami analysis and electron micrographs of structure analogs a layerlike crystalline structure is confirmed. The remaining amorphous interface may be caused by steric problems to incorporate a molecule in one of the neighboring crystals. If there is not enough space between

both it is impossible to reorient the stiff molecules in the direction necessary for crystallization. Then the dimension of the interface is limited to the molecule dimension of about 1.5 nm. This is in the same order of magnitude as the thickness of the mobile amorphous layers in semicrystalline PET.²⁸

For both, the semicrystalline low-molecular-weight compound and the semicrystalline PET a shift of the calorimetric glass transition temperature of about 15 K compared to that of an amorphous sample and a slowing down of the dielectric α -relaxation was observed. This effect seems to be a consequence of the spatial confinement and not caused by the chain structure of the polymer.

V. CONCLUSIONS

Dielectric relaxation measurements can be used as a powerful tool to characterize the changes occurring in glass forming systems during isothermal crystallization in real time. The changes observed in the dielectric relaxation process during crystallization can be phenomenologically described in terms of the Havriliak–Negami approximation. The shift of the peak position to higher temperatures (lower frequencies) can be related to spatial confinement in a system where the molecules of the glass forming fraction have the same interaction with the surface of the crystallites as in the amorphous fraction itself. The broadening of the α -relaxation can not be easily interpreted as a confinement effect. The effect is much more pronounced in semicrystalline polymers and may be caused by the chain structure.

ACKNOWLEDGMENTS

This work has been supported by the DFG (J.D. and M.P.) and the Hanns-Seidel-Stiftung (J.H.). We would like to thank Mrs. G. Marlow for careful DSC measurements and Dr. A. Schönhals (Berlin) and Dr. P. Dobbert (Rostock) for helpful comments and suggestions.

- ¹N. G. McCrum, B. E. Read, and G. Williams, *Anelastic and Dielectric Effects in Polymeric Solids* (Wiley, London, 1967).
- ²J. C. Coburn and R. H. Boyd, *Macromolecules* **19**, 2238 (1986).
- ³C. Schick, B. Stoll, J. Schawe, A. Roger, and M. Gnoth, *Prog. Colloid Polym. Sci.* **85**, 148 (1991).
- ⁴T. A. Ezquerro, F. J. Baltacalleja, and H. G. Zachmann, *Polymer* **35**, 2600 (1994).
- ⁵A. T. Ezquerro, J. Majszczyk, J. F. Baltacalleja, E. Lopezcabarcos, H. K. Gardner, and S. B. Hsiao, *Phys. Rev. B* **50**, 6023 (1994).
- ⁶H. Suzuki, J. Grebowicz, and B. Wunderlich, *Br. Polym. J.* **17**, 1 (1985).
- ⁷V. B. F. Mathot, *Calorimetry and Thermal Analysis of Polymers* (Hanser, Munich, 1994).
- ⁸E. Donth, *J. Non-Cryst. Solids* **53**, 325 (1982).
- ⁹J. Jäckle, *J. Non-Cryst. Solids* **172**, 104 (1994).
- ¹⁰M. Pötter, H. Dehne, H. Reinke, J. Dobbertin, and C. Schick, *Mol. Cryst. Liq. Cryst.* (in press).
- ¹¹F. Kremer, D. Boese, G. Meier, and E. W. Fischer, *Prog. Colloid Polym. Sci.* **80**, 129 (1989).
- ¹²S. Havriliak and S. Negami, *J. Polym. Sci., Part C: Polym. Symp.* **14**, 99 (1966).
- ¹³E. Schlosser and A. Schönhals, *Colloid Polym. Sci.* **267**, 963 (1989).
- ¹⁴G. P. Johari and M. Goldstein, *J. Chem. Phys.* **53**, 2372 (1970).
- ¹⁵C. A. Angell, *J. Non-Cryst. Solids* **131**, 13 (1991).
- ¹⁶R. Böhmer and C. A. Angell, *Phys. Rev. B* **45**, 10091 (1992).
- ¹⁷P. Huo and P. Cebe, *Macromolecules* **25**, 902 (1992).
- ¹⁸J. Dobbertin, A. Hensel, and C. Schick, *J. Therm. Anal.* **47**, 1027 (1996).
- ¹⁹M. Avrami, *J. Chem. Phys.* **7**, 1103 (1939); **8**, 212 (1940); **9**, 177 (1941).
- ²⁰H. G. Zachmann, *Fortschr. Hochpolym.-Forsch.* **3**, 581 (1964).
- ²¹U. Koy, H. Dehne, M. Gnoth, and C. Schick, *Thermochim. Acta* **229**, 299 (1993).
- ²²C. L. Jackson and G. B. McKenna, *J. Non-Cryst. Solids* **131**, 221 (1991).
- ²³P. Pissis, D. Daoukakidiamanti, L. Aspekis, and C. Christodoulides, *J. Phys.* **6**, L325 (1994).
- ²⁴J. Schüller, Y. B. Melnichenko, R. Richert, and E. W. Fischer, *Phys. Rev. Lett.* **73**, 2224 (1994).
- ²⁵M. Arndt, R. Stannarius, H. Groothues, E. Hempel, and F. Kremer, *Phys. Rev. Lett.* **79**, 2077 (1997).
- ²⁶J. L. Keddie, R. A. L. Jones, and R. A. Cory, *Europhys. Lett.* **27**, 59 (1994).
- ²⁷J. A. Forrest, K. Dalnokiveress, J. R. Stevens, and J. R. Dutcher, *Phys. Rev. Lett.* **77**, 2002 (1996).
- ²⁸C. Schick and E. Donth, *Phys. Scr.* **43**, 423 (1991).